Organometallic Chemistry | *Hot Paper*

The Missing Parent Compound $[(C_5H_5)Fe(\eta^5\text{-}P_5)]$: Synthesis, Characterization, Coordination Behavior and Encapsulation

Claudia Heinl, Eugenia Peresypkina, Gábor Balázs, Eric Mädl, Alexander V. Virovets, and Manfred Scheer*[a]

Dedicated to Prof. Otto J. Scherer in honor for his seminal achievements in pentaphosphaferrocene chemistry

Abstract: The so far missing parent compound of the large family of pentaphosphaferrocenes $[CpFe(\eta^5\text{-}P_5)]$ (**1b**) was synthesized by the thermolysis of $[CpFe(CO)_2]_2$ with P_4 using the very high-boiling solvent diisopropylbenzene. It was comprehensively characterized by, inter alia, NMR spectroscopy, single crystal X-ray structure analysis, cyclic voltammetry and DFT computations. Moreover, its coordination behavior towards Cu^I halides was explored, revealing the unprecedented 2D polymeric networks $[\{CpFe(\eta^{5:1:1:1:1}\text{-}P_5)\}Cu_2(\mu\text{-}X)_2]_n$ (**2a**: X = Cl, **2b**: X = Br) and $[\{CpFe(\eta^{5:1:1}\text{-}P_5)\}Cu(\mu\text{-}I)]_n$ (**3**) and even the first *cyclo*-P_5-containing 3D coordination polymer $[\{CpFe(\eta^{5:1:1}\text{-}P_5)\}Cu(\mu\text{-}I)]_n$ (**4**). The sandwich complex **1b** can also be incorporated in nano-sized supramolecules based on $[Cp^*Fe(\eta^5\text{-}P_5)]$ (**1a**) and CuX (X = Cl, Br, I): $[CpFe(\eta^5\text{-}P_5)]@[\{Cp^*Fe(\eta^5\text{-}P_5)\}_{12}(CuX)_{20\text{-}n}]$ (**5a**: X = Cl, $n = 2.4$; **5b**: X = Br, $n = 2.4$; **5c**: X = I, $n = 0.95$). Thereby, the formation of the CuI-containing fullerene-like sphere **5c** is found for the first time.

Introduction

The establishment of organometallic chemistry as a distinct field of chemistry is—to a large extent—owed to the discovery and structure determination of the ferrocene molecule $[Fe(\eta^5\text{-}C_5H_5)_2]$ in 1951,[1] for which E. O. Fischer and G. Wilkinson were awarded the Noble Prize in 1973.[2] Beside their application as a reference redox system (Fc/Fc^+),[3] ferrocene derivatives play an important role for example, in asymmetric catalysis,[4] polymer chemistry[5] and for magnetic materials.[6] These derivatives can not only be varied in their functionalization pattern, but also in the substitution of the methine moieties of the C_5H_5 group by isolobal heteroatoms. Since a P atom is isolobal to a CH fragment, the introduction of phosphorus atoms into the cyclopentadienyl ligand affords the class of phosphaferrocenes.[7] Among them, the Cp*-substituted pentaphosphaferrocene $[Cp^*Fe(\eta^5\text{-}P_5)]$ ($Cp^* = C_5Me_5$) (**1a**), containing a *cyclo*-P_5 ligand, is of special interest. First published in 1987 by Scherer et al.,[8] it shows a remarkable similarity to ferrocene, since it was possible to oxidize, reduce and substitute on the *cyclo*-P_5 ring.[9] Moreover, it has become an important building block not only in organometallic,[10] but also in coordination and supramolecular chemistry especially for the formation of 1D and 2D polymers.[11]

Of special interest is its ability to act as a building block for the formation of spherical supramolecules with fullerene topology by a self-assembly process with CuX (X = Cl, Br).[12] Furthermore, these spheres can encapsulate molecules such as **1a** itself (Figure 1a),[12e,h] ferrocene (Figure 1b),[12c] *o*-carborane[12a,f] and also C_{60}.[12g] These reactions turned out to be very sensitive to many parameters such as stoichiometry, solvent, concentration and the used halide. Hence, also the nature of the Cp^R ligand in the pentaphosphaferrocene should profoundly affect

[a] Dr. C. Heinl, Dr. E. Peresypkina, Dr. G. Balázs, Dr. E. Mädl, Dr. A. V. Virovets, Prof. Dr. M. Scheer
Institut für Anorganische Chemie
Universität Regensburg
93040 Regensburg (Germany)
E-mail: Manfred.scheer@ur.de

Supporting information and the ORCID identification number(s) for the author(s) of this article can be found under: https://doi.org/10.1002/chem.202100203.

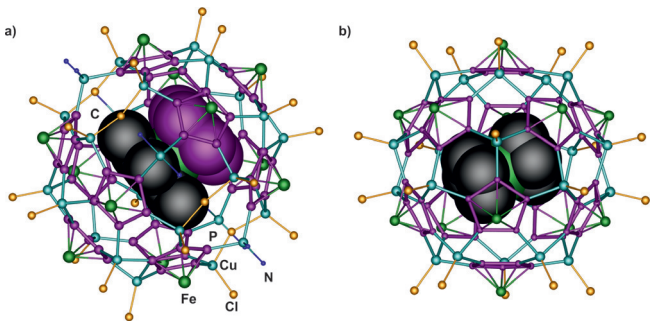

Figure 1. Fullerene-like spheres based on **1a** and CuCl: a) 90-vertex supramolecule incorporating **1a**; b) 80-vertex supramolecule incorporating $[FeCp_2]$.

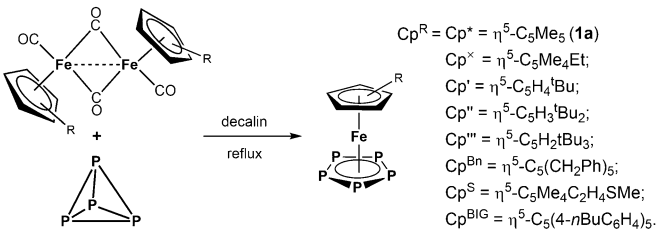

Scheme 1. General procedure for the synthesis of pentaphosphaferrocenes.

the coordination behavior. Due to their rather straightforward synthesis in decalin as solvent (Scheme 1), a huge variety of pentaphosphaferrocenes is known so far with $Cp^R = Cp^\times = \eta^5$-$C_5Me_4Et$;[13] $Cp' = \eta^5$-C_5H_4tBu;[14] $Cp'' = \eta^5$-$C_5H_3tBu_2$;[13] $Cp''' = \eta^5$-$C_5H_2tBu_3$;[15] $Cp^{Bn} = \eta^5$-$C_5(CH_2Ph)_5$;[16] $Cp^S = \eta^5$-$C_5Me_4C_2H_4SMe$;[15] $Cp^{BIG} = \eta^5$-$C_5(4\text{-}nBuC_6H_4)_5$.[17]

In view of the large variety of Cp^R-substituted pentaphosphaferrocenes, it is surprising that the parent compound [CpFe(η^5-P_5)] (**1 b**) with an unsubstituted Cp ligand has never been reported. Especially this sandwich complex is of great interest as building block itself, as guest for the encapsulation in fullerene-like supramolecules and as general starting material in organometallic chemistry.

Although several detailed DFT computational studies predicted **1 b** to be stable,[18] its synthesis remained an insuperable challenge. There is evidence that several attempts were in fact made to synthesize it. However, the use of decalin as solvent does not lead to the formation of **1 b**, but to a tetranuclear iron cluster (Scheme 2).[19] Recently, we have shown that by using a higher-boiling solvent, [Cp*Fe(η^5-P_5)] as well as triple decker sandwich complexes can be obtained in much better yields than by earlier reported procedures and, by this means, for example, the hitherto unknown parent compound [$(CpMo)_2(\mu,\eta^{6:6}$-$P_6)$] could also be synthesized for the first time.[20]

Herein, we report on the first synthesis and the comprehensive characterization of the parent pentaphosphaferrocene [CpFe(η^5-P_5)] (**1 b**). In order to compare its coordination behavior with that of the substituted pentaphosphaferrocenes, its reactivity towards Cu^I halides was studied. Among the obtained products is the first 3D polymer in the *cyclo*-P_5 ligand coordination chemistry. Furthermore, the ability of **1 b** was discovered

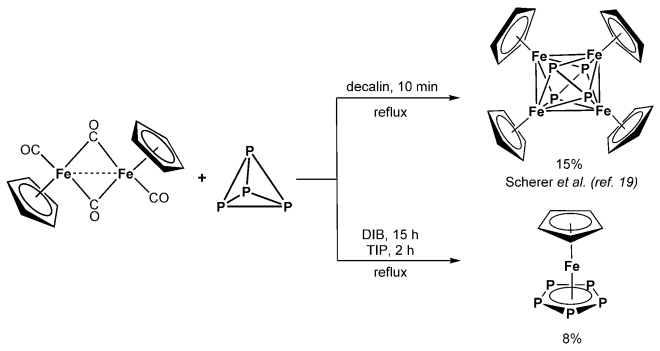

Scheme 2. Thermolysis reaction of $[CpFe(CO)_2]_2$ with P_4.

to act as a template for the formation of unprecedented inorganic nano-sized spheres.

Results and Discussion

Synthesis and characterization of 1 b

For the synthesis of all hitherto synthesized pentaphosphaferrocenes a similar route was applied (Scheme 1). The thermolysis of $[Cp^RFe(CO)_2]_2$ with P_4 in decalin and subsequent chromatographic work-up afford the desired complex as a green solid. When, however, this strategy is transferred to the Cp derivative the tetranuclear iron cluster $[(CpFe)_4(P_2)_2]$ is obtained exclusively (Scheme 2).[19]

Since thermal conversion depends on the applied temperature, $[CpFe(CO)_2]_2$ was allowed to react with P_4 in 1,3-diisopropylbenzene with a higher boiling point in comparison to that of decalin (DIB, bp = 203 °C; decalin: bp = 187–196 °C). Interestingly, this rather small temperature increase was, most likely, the decisive factor to produce the unsubstituted parent compound **1 b** as sole product according to $^{31}P\{^1H\}$ NMR spectroscopy for the first time (Scheme 2). However, the aromatic character of the used solvent might also be crucial for the formation of **1 b**. The latter was purified by chromatographic workup to give a green powder in 8% yield. To investigate whether the yield can be enhanced by a further increase of the temperature, the reaction was performed in 1,3,5-triisopropylbenzene (TIP, bp = 232–236 °C). **1 b** can, in fact, be isolated after a significantly shorter reaction time of 2 hours, with the isolated yield remaining similar, due to the chromatographic workup.

Complex **1 b** is poorly soluble in aliphatic solvents such as *n*-hexane, moderately soluble in toluene and CH_2Cl_2 and insoluble in CH_3CN. As expected, the ^1H NMR spectrum of **1 b** shows one singlet at $\delta = 3.39$ ppm, which is upfield shifted compared to [$FeCp_2$] ($\delta = 4.04$ ppm).[21] In the $^{31}P\{^1H\}$ NMR spectrum, one singlet appears at $\delta = 169.5$ ppm, thus revealing the equivalence of all the P atoms. This signal exhibits one of the farthest downfield shifts for the pentaphosphaferrocene compounds (signals range from $\delta = 152.8$ ppm for [$Cp^\times Fe(\eta^5$-$P_5)$][13] to $\delta =$ 173.6 for [$Cp^{BIG}Fe(\eta^5$-$P_5)$][17]), which therefore does not go hand in hand with the steric bulk, unlike previously assumed.[16,17] Furthermore, complex **1 b** sublimes at 80 °C/10^{-3} mbar, just as **1 a** did.[8]

By layering a CH_2Cl_2 solution of **1 b** with CH_3CN in a thin Schlenk tube, **1 b** crystallizes as green prisms in the monoclinic space group $P2_1/m$. Its molecular structure reveals a sandwich complex with η^5-coordinated rings in a perfect eclipsed conformation, which is in accordance with all theoretical predictions (Figure 2).[18] In contrast, due to the steric demand of the methyl substituents, the Cp* derivative **1 a** deviates from the eclipsed conformation by 11.6(1)°.[11b] The interplanar angle of **1 b** is close to zero (0.56(8)°) and the angle $Cp_{(centroid)}$-Fe-$P_{5(centroid)}$ of 179.87(4) with both of them revealing a perfect sandwich complex almost free of distortion. The molecule **1 b** lies in a mirror plane (C_s point symmetry) that bisects both Cp and P_5 rings (Figure 2) similarly to Cp_2Ru,[22] Cp_2Os[23] and the low-temperature orthorhombic modification of Cp_2Fe.[24] In

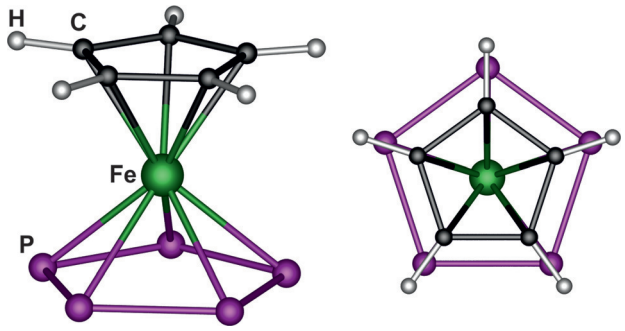

Figure 2. Molecular structure of **1 b** in the crystal (side and top view).

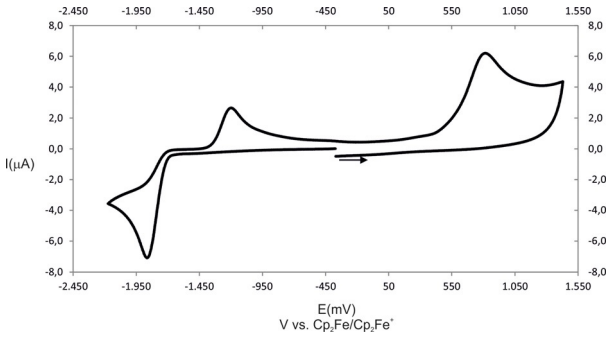

Figure 3. Cyclic voltammogram of **1 b** in CH_2Cl_2/nBu$_4$NPF$_6$ solution at r.t. and $\nu = 0.1$ Vs^{-1}.

contrast to ferrocene,[24] **1 b** demonstrates no phase transition in the temperature range of 123 K–298 K. The diffraction experiment at room temperature of a single crystal of **1 b** showed only increased thermal motion (see Supporting Information for details). A comparison of selected bond lengths of **1 b** with optimized geometries based on DFT computations as well as with experimental data of **1 a** is given in Table 1. It can be stated that all predicted values are in part significantly longer than the experimentally observed ones. Furthermore, π-stacking interactions are present, since the **1 b** molecules are arranged into head-to-tail chains (along the *c* axis) via Cp···*cyclo*-P$_5$ interactions with interplanar distances of 3.71 Å or 3.78 Å at $T = 123$ K or r.t., respectively (see Supporting Information for detail).

Table 1. Selected bond lengths and reported DFT optimized geometries of **1 b** at 123 K (l.t.), **1 b** at 298 K (r.t.) and **1 a**, respectively.

Bond lengths [Å]	Fe–Cp^R $_{(centroid)}$	Fe–P$_5$ $_{(centroid)}$	P–P$_{average}$
1 b	1.693(1)$^{l.t.}$	1.536(1)$^{l.t.}$	2.113(3)$^{l.t.}$
	1.698(1)$^{l.t.}$	1.536(1)$^{r.t.}$	2.10(1)$^{r.t.}$
Katsyuba et al.[17a]	1.706	1.623	2.148
Padma Malar[17b]	1.705	1.624	2.148
Frenking et al.[17c]	1.716	1.599	2.163
Frison et al.[17d]	1.695	1.578	2.137
this work	1.712	1.585	2.127
1 a[10b]	1.720(1)	1.535(1)	2.120(2)

R. Winter et al. investigated the interesting redox behavior of the Cp* derivative [Cp*Fe(η^5-P$_5$)] (**1 a**) and stated a one-electron oxidation and reduction, which is reversible at high scan rates.[25] However, the resulting complexes are not stable and readily dimerize to give [**1 a**$_2$]$^{2+}$ and [**1 a**$_2$]$^{2-}$, respectively. Their proposed structures were finally confirmed experimentally by our group.[9] For a comparison, the electrochemical investigations were also performed for **1 b** (Figure 3). Cyclic voltammetry data at a sweep rate of 0.1 Vs^{-1} reveal an irreversible oxidation at a peak potential of 0.8 V (0.6 V for **1 a**). Contrary to **1 a**, no coupled cathodic signal appears, which might be attributed to a dimeric species. Most likely, its stabilization by the sterically more demanding Cp* ligand is crucial, therefore the signal cannot be observed for **1 b**. However, the reduction behavior of **1 b** is in line with the results for **1 a**. A reduction wave at a peak potential of −1.86 (−2.05 V for **1 a**) as well as the corresponding anodic signal at −1.20 V (−1.34 V for **1 a**) constitute a chemically reversible couple.

DFT computations[26] of the electronic structure of **1 b** show an orbital ordering that resembles that of **1 a**[27] (Figure 4). As compared with **1 a**, in **1 b**, the Highest Occupied Molecular Orbital (HOMO) as well as the Lowest Unoccupied Molecular Orbital (LUMO) lie slightly lower in energy than in **1 a**, rendering **1 b** a weaker donor, but better acceptor (for the comparative energy level diagram of **1 a** and **1 b**, see Supporting Information). The HOMO–LUMO gap in **1 b** is 4.34 eV, whereas in **1 a** it is 4.48 eV. The difference in the relative energy of the frontier orbitals in **1 a** and **1 b** is in line with the results of the CV measurements.

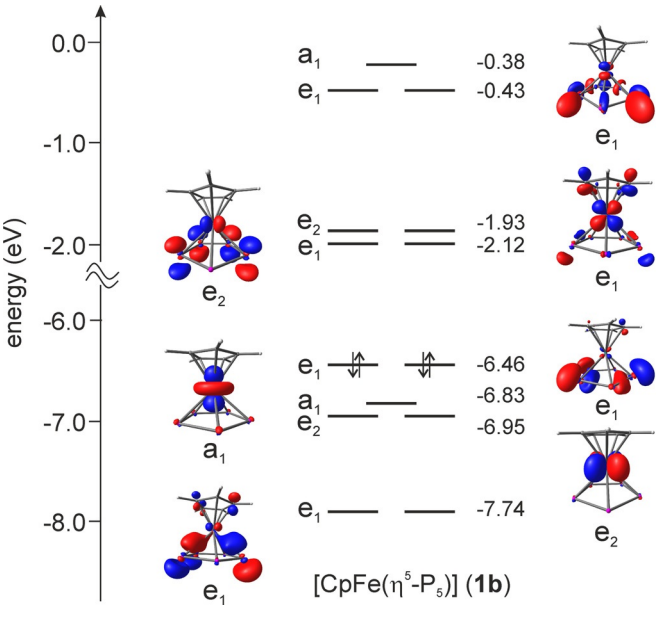

Figure 4. Energy level diagram for **1 b** calculated at the B3LYP/6-31++G(3df,3pd) level of theory.

Coordination behavior of 1 b towards Cu^I halides

Due to the lone pairs on the P$_5$ ring in combination with its outstanding five-fold symmetry, pentaphosphaferrocenes represent excellent building blocks in supramolecular chemistry. Hence, the coordination behavior of **1 b** towards Cu^I halides

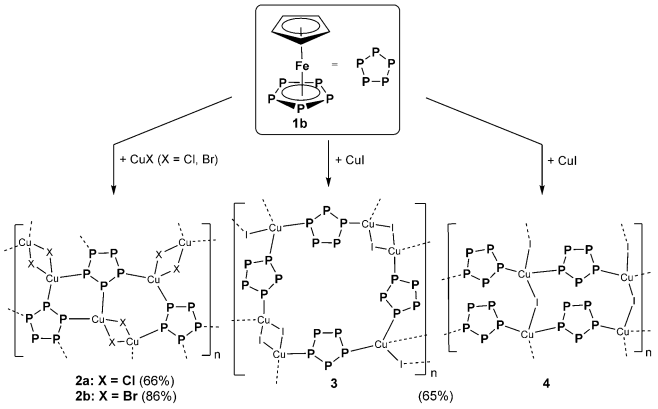

Scheme 3. Coordination behavior of **1b** towards Cu^{I} halides (Yields in parenthesis).

was investigated (Scheme 3). A green solution of **1b** in CH_2Cl_2 or toluene is layered with a colorless solution of CuX (X = Cl, Br, I) in CH_3CN in a very thin Schlenk tube. The phase boundary turns yellow-orange and small crystals of $[\{CpFe(\eta^{5:1:1:1:1}\text{-}P_5)\}Cu_2(\mu\text{-}X)_2]_n$ (**2a**: X = Cl, **2b**: X = Br), $[\{CpFe(\eta^{5:1:1}\text{-}P_5)\}Cu(\mu\text{-}I)]_n$ (**3**) and $[\{CpFe(\eta^{5:1:1}\text{-}P_5)\}Cu(\mu\text{-}I)]_n$ (**4**), respectively, start to grow after a few hours already. Due to the same (in)solubility, the CuI-containing polymers **3** and **4** cannot be separated. Unfortunately, regardless of several attempts, a selective synthesis is not feasible either, since they contain the same molar ratio of **1b** and CuI. Based on the different colors, orange for **3** and red for **4**, only a manual separation by crystal picking separates the products.

Compounds **2a** and **2b** are isostructural and crystallize as very thin orange plates in the triclinic space group $P\bar{1}$. Single-crystal X-ray structure analysis reveals 2D polymers with a 1,2,3,4-coordination mode of the *cyclo*-P_5 ligand (Figure 5a). The coordination of four P atoms of the ring occurred before in three previous examples, namely $[\{Cp^{R}Fe(\eta^5\text{-}P_5)\}(CuI)_3]_n$ (Cp^{R} = Cp*, Cp^{Bn})[11c,28] and $[\{Cp^{*}Fe(\eta^5\text{-}P_5)\}\{Cu(GaCl_4)\}_2]_n$.[11d] However, **2a** and **2b** differ from these examples in their connectivity and show an unprecedented structural motif. In addition to $\{Cu_2P_4\}$ hexagons and $\{Cu_2X_2\}$ squares, also seven-membered $\{Cu_3P_4\}$ rings are present. This linking pattern forms a planar 2D sheet structure with an orientation of the {CpFe} units alternating upwards and downwards. Note that they now deviate from the eclipsed conformation of the Cp ligand to the *cyclo*-P_5 unit by ≈14°. Interestingly, **2a**,**b** represent a novel layer topology for pentaphosphaferrocenes with 3-coordinated Cu^{+} and 4-coordinated **1b** units serving as nodes and halide spacers (see Supporting Information).[29]

Compound **3** crystallizes in the monoclinic space group $P2_1/c$. Its 2D polymeric network consists of connected rectangles of **1b** and four-membered Cu_2I_2 rings (Figure 5b). Two of the four {FeCp} units per rectangle are orientated towards each other. The *cyclo*-P_5 moieties show a 1,3-coordination mode, which had been unknown for pentaphosphaferrocenes in coordination polymers for a long time. Some years ago, we were able to obtain two examples, $[\{Cp^{*}Fe(\eta^5\text{-}P_5)\}(CuI)]_n$[11c] and $[\{Cp^{BIG}Fe(\eta^5\text{-}P_5)\}Ag]_n[Al\{OC(CF_3)_3\}_4]_n$,[11d] both, however, forming infinite chain 1D polymers. The only example of a supramolecule based on a 1,3-coordination mode of $[Cp''Fe(\eta^5\text{-}P_5)]$ with—interestingly, a minimum amount of metal cations—has been obtained only very recently.[30] In contrast, **3** forms two-dimensional layers. When the bridging iodine atoms and the 1,3-coordinated **1b** molecules are treated as spacers and the Cu atoms as nodes of the polymeric structure, the honeycomb **hcb** topology of the layer becomes evident.[29,31]

Compound **4** crystallizes as red prisms in the orthorhombic space group $Pna2_1$. Remarkably, it is a constitutional isomer of **3**, having the same sum formula $[\{CpFe(\eta^5\text{-}P_5)\}Cu(\mu\text{-}I)]_n$ but different connectivity, representing the first example of a 3D pentaphosphaferrocene-based polymer. This is astonishing, since all obtained pentaphosphaferrocene-based polymers are either 1D or 2D.[11] In **4**, two P atoms per P_5 ring are connected to Cu, resulting in a 1,3-coordination mode as it is observed in **3** (Figure 6). As in **3**, Cu possesses the tetrahedral environment with the bridging coordination of iodide. In contrast to **3**, no $\{Cu_2I_2\}$ rings but infinite {CuI} zigzag chains are formed in **4** (Figure 6). Its net topology can be assigned to the **dia** type,[29,32] which is for example, known for diamond (Figure 7).

Among these polymers, π-stacking interactions, similar to the ones found in **1b**, do not occur. Despite rather short inter-

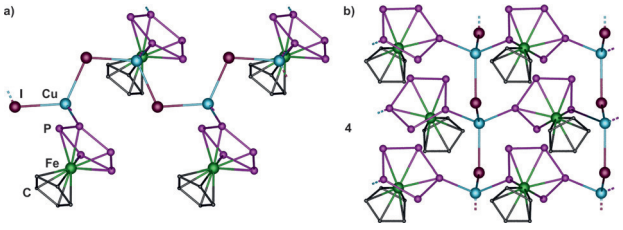

Figure 6. Sections of the 3D polymeric structure of **4**: view along the crystallographic a) *a* axis and b) *b* axis. Hydrogen atoms are omitted for clarity.

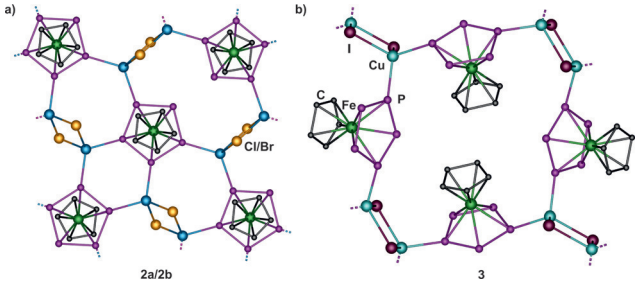

Figure 5. Sections of the 2D polymeric structures of a) **2a**/**2b** and b) **3**. Hydrogen atoms are omitted for clarity.

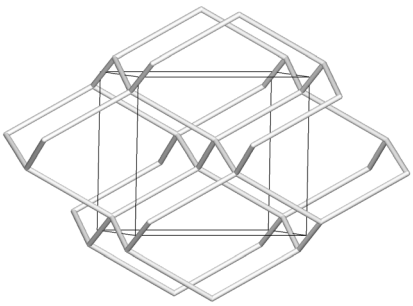

Figure 7. dia topology in **4**.

layer distances of 3.22 Å in **2a** and 3.27 Å in **2b**, the layers are mutually shifted and do not afford a direct contact of the π-systems. In both **3** and **4**, the π-systems are not parallel, and all contacts involving P atoms are within the range of van der Waals interactions.

All four coordination polymers are insoluble in common solvents such as hexane, toluene, CH_2Cl_2, CH_3CN, Et_2O and thf. They can only be dissolved in pyridine, albeit accompanied by complete fragmentation. Hence in the ^1H and $^{31}P\{^1H\}$ NMR spectra, respectively, only the singlet for **1b** can be detected.

Inclusion of 1b in fullerene-like spheres

Compound **1b** does not only represent an interesting building unit, but is also excellently suited for the encapsulation into pentaphosphaferrocene-based supramolecules. Recently, we were able to show that ferrocene [$FeCp_2$] can be incorporated in an 80-vertex sphere consisting of 12 molecules of **1a** and 20 CuCl units.[12c] The scaffold only consists of five- (P_5) and six-membered {Cu_2P_4} rings and shows I_h-C_{80} fullerene topology. Also, pentaphosphaferrocene **1a** itself acts as a template and is enclosed by a 90-vertex supramolecule.[12e,h] This sphere exhibits a slightly larger scaffold due to the larger size of **1a**. More tellingly, one can imagine the 80-vertex ball as being divided into two equal half shells with a [{$Cu(CH_3CN)_2$}$_5X_5$] (X = Cl, Br) belt combining them. Since the size of **1b** is in between, the question arises as to which host will be the preferred one.

To answer this question, a dark green solution of **1a** and **1b** in CH_2Cl_2 (molar ratio **1a**:**1b** = 9:1) is layered with a colorless solution of CuX (X = Cl, Br, I), respectively. Remarkably, in all three reactions, black rhombohedra of [$CpFe(\eta^5$-$P_5)$]@[{$Cp^*Fe(\eta^5$-$P_5)$}$_{12}$($CuX)_{20-n}$] (**5a**: X = Cl, n = 2.4; **5b**: X = Br, n = 2.4; **5c**: X = I, n = 0.95) are formed immediately.[33] All three compounds are isostructural and crystallize in the trigonal space group $R\bar{3}$. In their structures, one molecule of **1b** is incorporated into the smaller 80-vertex nanoball regardless of which halide is used (Figure 8), showing the distinctly preferred encapsulation of the pentaphosphaferrocene guest **1b**. Note that **5c** displays the first fullerene-analogue containing copper iodide. Most previous attempts starting with CuI and **1a** resulted in the formation of polymeric products. Merely few P_5-based supramolecules with CuI are known, without any of them, however, following the fullerene topology.[12b,h,28] Therefore, the selective formation of **5c** is very remarkable and reveals the perfect template properties of **1b**.

The host molecules in **5a–c** consist of 12 moieties of **1a**, which show an all-P coordination mode to copper. The complete 80-vertex scaffold would contain 20 CuX (X = Cl, Br, I) units forming 30 {Cu_2P_4} six-membered rings. However, in all three spherical compounds, the scaffold exhibits some number of CuX vacancies. This phenomenon was also observed for a similar system with *o*-carborane and ferrocene as guests.[12a,h] As a consequence, the ideal number of 20 in the $Cu_{20}P_{60}$ scaffold is reduced per supramolecule to 15.9 for **5a**, 17.4 for **5b** and 16.4 for **5c** (Figure 8b) giving rise to non-stoichiometric solid solutions of metal-deficient supramolecules. Some solvent CH_2Cl_2 molecules point into the vacant holes in the copper-

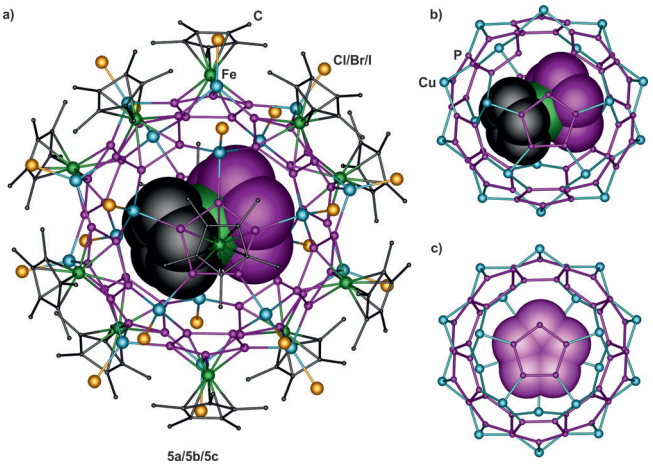

Figure 8. a) Molecular structures of **5a–c** in the crystal with one possible orientation of the disordered guest molecule **1b**. Hydrogen atoms are omitted for clarity; metal-deficient inorganic scaffold of the supramolecules with incorporated **1b** in b) side and c) top view.

phosphorus scaffold that can cause a partial ordering of supramolecules, similar to toluene molecules.[12a] Another consequence of these 'holes' for the adjacent *cyclo*-P_5 ligands is the stochastic reduction of the pentacoordination, in most cases to a tetra- or three-coordination to copper.

The outer diameter of all three supramolecules is 2.12 nm and does not depend on the nature of the halide, since the Cp* ligands protrude furthest. The inner diameters are determined by the distance between opposite *cyclo*-P_5 ligands and are therefore identical with a value of 0.77 nm. These dimensions are in good agreement with previously obtained 80-vertex spheres.[12a,c,f] Furthermore, the spherical cavity shows the appropriate size for one molecule of **1b** (0.70 × 0.67 nm).

The guest molecule is present in each cavity of the supramolecules **5a–c** as proved by the occupancy factors of the Fe atoms in the center. All other atoms are severely disordered over twelve positions even at 10 K (**5a**), partly related by symmetry (see Supporting Information for details). In contrast to a ferrocene encapsulation where the distinctive face-to-face orientation of Cp ligands towards the *cyclo*-P_5 ligands of the host points out possible Cp···P_5 π-stacking host–guest interactions,[12h] the *cyclo*-P_5 ligands of the **1b** guest do not demonstrate any preferable orientation with respect to the host supramolecule. Angles between the P_5 aromatic systems belonging to **1b** and the host molecules **5a–c** vary in a range between 0.8(3)° and 23.5(9)° with the corresponding P···P contacts being beyond the sum of van-der-Waals radii of 3.6 Å (see Supporting Information for details).[34]

The supramolecules **5a–c** are all obtained by diffusion reactions and their synthesis can always be accompanied by the formation of polymeric networks [$Cp^*Fe(\eta^5$-$P_5)(CuX)]_n$[11a] (X = Cl, Br, I). In addition, for X = Cl, Br, also the 90-vertex spheres [$Cp^*Fe(\eta^5$-$P_5)$]@[{$Cp^*Fe(\eta^5$-$P_5)$}$_{12}$($CuX)_{25}$($CH_3CN)_{10}$][12e] can be formed within these self-assembly processes. However, a precise monitoring during the diffusion process revealed that, for X = Cl, Br, black rhombohedra of **5a**/**5b** crystallize at the phase boundary first. After approximately one to two days, brownish

plates of $[Cp^*Fe(\eta^5\text{-}P_5)(CuX)]_n$ are visible at the bottom of the Schlenk tube. Finally, after complete diffusion, rods of the crystalline phase containing 90-vertex supramolecules start to appear. Therefore, to obtain pure **5a**, one has to collect the crystals as soon as possible only from the Schlenk wall with a spatula (see Supporting Information). That way, pure **5a** is obtained in still very good crystalline yields of 64%. Unfortunately, this separation procedure is not possible for X = I, since crystals of **5c** and $[Cp^*Fe(\eta^5\text{-}P_5)(CuI)]_n$ start to grow in the same areas concomitantly at random.

All obtained supramolecules are completely insoluble in common solvents such as hexane, toluene, CH_3CN, Et_2O and thf, but can be dissolved in pyridine at the cost of fragmentation. Therefore, in the corresponding ^1H and $^{31}P\{^1H\}$ NMR spectra, only signals of the starting complexes **1a** and **1b** are observed, additionally proving the encapsulation of **1b**. On the other hand, this also means that the encapsulated pentaphosphaferrocene **1b** can be released by disassembling of its host.

Surprisingly and contrary to previously reported 80-vertex supramolecules, which are completely insoluble in any organic solvent,[12c,f,h] **5a** and **5b** are slightly soluble in CH_2Cl_2 (but still very poorly). Thus, a characterization by NMR spectroscopy is enabled. In the $^{31}P\{^1H\}$ NMR spectrum of **5a**, three very broad signals at $\delta = 70$, 76 and 103 ppm, one sharp singlet at $\delta =$ 152.1 ppm and one slightly broadened singlet at $\delta =$ 170.5 ppm can be observed. According to a detailed NMR study of soluble supramolecules with Cp^{Bn}-based pentaphosphaferrocene, the broad signals can be assigned to the coordinated P atoms of spheres with varying metal-deficiency.[35] In addition, a small amount of **1a** might be released, causing the singlet at $\delta = 152.1$ ppm. Due to the broadening, the singlet at $\delta = 170.5$ ppm is assigned to the encapsulated complex **1b**, thus being slightly downfield-shifted compared to free **1b** (in CD_2Cl_2: $\delta = 168.6$ ppm). This observation is in contrast to previously reported guest molecules, which all show a slight shift to higher field. Therefore, **1b** displays the first template which might rather act as an electron donor. The quality of the $^{31}P\{^1H\}$ NMR spectrum of the analogous compound **5b** is already quite poor, since its solubility is even worse. Nevertheless, also two singlets for **1a** and **1b** as well as one very broad signal for **5b** can be observed. Other broad signals, as they were observed for **5a**, can only be adumbrated and disappear below the noise floor.

Conclusions

In summary, the first synthesis and comprehensive characterization of the parent pentaphosphaferrocene $[CpFe(\eta^5\text{-}P_5)]$ (**1b**) are presented. The replacement of decalin by the even higher-boiling solvents DIB or TIP makes the general route feasible for the formation of the so far missing example of a parent complex. The X-ray structure analysis reveals an eclipsed sandwich complex with slightly shorter bond lengths than the theoretically predicted ones. The DFT computations also reveal a slightly stronger acceptor and weaker donor ability, compared to the Cp* derivative **1a**. The cyclic voltammetry data show an irreversible oxidation and a reversible reduction. To investigate the coordination behavior of **1b**, it was reacted with CuX (X = Cl, Br, I). In all reactions, the formation of unprecedented 2D polymers (**2a**, **2b** and **3**) and even the first 3D polymer (**4**) based on pentaphosphaferrocene is observed. The networks **2a** and **2b** show a 1,2,3,4-coordination mode of the *cyclo*-P_5 ligand, whereas, in **3** and **4**, a 1,3-coordination is present. At the same time, no sign of the formation of **1b**-based supramolecules was observed. Furthermore, the incorporation of **1b** as a guest into 80-vertex nanoballs (**5a–c**) was examined. The host molecules differ in the halide and, for the first time, an iodine-containing supramolecule with fullerene topology is obtained. Its behavior in solution shows that **1b** remains incorporated in the host in CH_2Cl_2, whereas fragmentation and therefore the release of the template are observed in donor solvents such as pyridine. Moreover, **1b** displays the first template for fullerene topological spheres, showing to act as an electron donor to the overall host assembly. All in all, the influence of the unsubstituted parent Cp ligand is demonstrated: starting from different conditions during its synthesis through its deviating coordination behavior towards copper(I) to changes in its host-guest chemistry owing to its smaller size. Moreover, the successful synthesis of **1b** opens the possibility to explore the preference of organometallic transformations occurring either on the Cp or the *cyclo*-P_5 ligand, a fascinating comparison for future work.

Experimental Section

Crystallographic data: Deposition numbers 2054500 (**1b**), 2054499 (**1b r.t.**), 2049560 (**2a**), 2049561 (**2b**), 2049562 (**3**), 2049563 (**4**), 2054501 (**5a**), 2054504 (**5a 10K**), 2054503 (**5b**), 2054502 (**5c**) contain the supplementary crystallographic data for this paper. These data are provided free of charge by the joint Cambridge Crystallographic Data Centre and Fachinformationszentrum Karlsruhe Access Structures service.

Acknowledgements

This work was supported by the Deutsche Forschungsgemeinschaft (DFG) (project Sche 384/44-1). C.H. is grateful for a PhD fellowship of the Fonds der Chemischen Industrie. Parts of this research (project I-20160654) were carried out at PETRA III at DESY, a member of the Helmholtz Association (HGF). We thank Dr. A. Burkhardt and PD Dr. B. Dittrich for their assistance regarding the use of the beamline P11. Open access funding enabled and organized by Projekt DEAL.

Conflict of interest

The authors declare no conflict of interest.

Keywords: Cu^I halides · host–guest chemistry · parent pentaphosphaferrocene · phosphaferrocene · supramolecular chemistry

[1] a) T. J. Kealy, P. L. Pauson, *Nature* **1951**, *168*, 1039 – 1040; b) G. Wilkinson, M. Rosenblum, M. C. Whiting, R. B. Woodward, *J. Am. Chem. Soc.* **1952**, *74*, 2125 – 2126.

[2] G. Wilkinson, *Angew. Chem.* **1974**, *86*, 664 – 667.

[3] a) G. Gritzner, J. Kuta, *Pure Appl. Chem.* **1984**, *56*, 461 – 466; b) N. G. Connelly, W. E. Geiger, *Chem. Rev.* **1996**, *96*, 877 – 910.

[4] a) A. Togni, in *Metallocenes: Synthesis Reactivity Applications, Vol. 11* (Eds.: A. Togni, R. Halterman), Wiley-VCH, Weinheim, **1998**, pp. 685 – 718; b) C. J. Richards, A. J. Locke, *Tetrahedron: Asymmetry* **1998**, *9*, 2377 – 2407.

[5] a) T. Fukino, H. Joo, Y. Hisada, M. Obana, H. Yamagishi, T. Hikima, M. Takata, N. Fujita, T. Aida, *Science* **2014**, *344*, 499 – 504; b) Z. M. Hudson, I. Manners, *Science* **2014**, *344*, 482 – 483; c) P. Nguyen, P. Gomez-Elipe, I. Manners, *Chem. Rev.* **1999**, *99*, 1515 – 1548.

[6] a) I. P. Chang, K. C. Hwang, C.-S. Chiang, *J. Am. Chem. Soc.* **2008**, *130*, 15476 – 15481; b) H. Kumari, C. L. Dennis, A. V. Mossine, C. A. Deakyne, J. L. Atwood, *J. Am. Chem. Soc.* **2013**, *135*, 7110 – 7113.

[7] a) F. Mathey, A. Mitschler, R. Weiss, *J. Am. Chem. Soc.* **1977**, *99*, 3537 – 3538; b) L. Weber, *Angew. Chem. Int. Ed.* **2002**, *41*, 563 – 572; *Angew. Chem.* **2002**, *114*, 583 – 592.

[8] O. J. Scherer, T. Brück, *Angew. Chem Int. Ed.* **1987**, *26*, 59; *Angew. Chem.* **1987**, *99*, 59.

[9] a) M. V. Butovskiy, G. Balázs, M. Bodensteiner, E. V. Peresypkina, A. V. Virovets, J. Sutter, M. Scheer, *Angew. Chem. Int. Ed.* **2013**, *52*, 2972 – 2976; *Angew. Chem.* **2013**, *125*, 3045 – 3049; b) E. Mädl, M. V. Butovskii, G. Balázs, E. V. Peresypkina, A. V. Virovets, M. Seidl, M. Scheer, *Angew. Chem. Int. Ed.* **2014**, *53*, 7643 – 7646; *Angew. Chem.* **2014**, *126*, 7774 – 7777; c) E. Mädl, E. Peresypkina, A. Y. Timoshkin, M. Scheer, *Chem. Commun.* **2016**, *52*, 12298 – 12301.

[10] a) O. J. Scherer, T. Brück, G. Wolmershäuser, *Chem. Ber.* **1989**, *122*, 2049 – 2054; b) M. Detzel, T. Mohr, O. J. Scherer, G. Wolmershäuser, *Angew. Chem. Int. Ed.* **1994**, *33*, 1110 – 1112; *Angew. Chem.* **1994**, *106*, 1142 – 1144; c) B. Rink, O. J. Scherer, G. Wolmershäuser, *Chem. Ber.* **1995**, *128*, 71 – 73.

[11] a) J. Bai, A. V. Virovets, M. Scheer, *Angew. Chem. Int. Ed.* **2002**, *41*, 1737 – 1740; *Angew. Chem.* **2002**, *114*, 1808 – 1811; b) M. Scheer, L. J. Gregoriades, A. V. Virovets, W. Kunz, R. Neueder, I. Krossing, *Angew. Chem. Int. Ed.* **2006**, *45*, 5689 – 5693; *Angew. Chem.* **2006**, *118*, 5818 – 5822; c) F. Dielmann, A. Schindler, S. Scheuermayer, J. Bai, R. Merkle, M. Zabel, A. V. Virovets, E. V. Peresypkina, G. Brunklaus, H. Eckert, M. Scheer, *Chem. Eur. J.* **2012**, *18*, 1168 – 1179; d) C. Heindl, S. Heinl, D. Luedeker, G. Brunklaus, W. Kremer, M. Scheer, *Inorg. Chim. Acta* **2014**, *422*, 218 – 223; e) M. Fleischmann, L. Duetsch, M. E. Moussa, A. Schindler, G. Balázs, C. Lescop, M. Scheer, *Chem. Commun.* **2015**, *51*, 2893 – 2895; f) M. Fleischmann, S. Welsch, H. Krauss, M. Schmidt, M. Bodensteiner, E. V. Peresypkina, M. Sierka, C. Groeger, M. Scheer, *Chem. Eur. J.* **2014**, *20*, 3759 – 3768.

[12] a) E. V. Peresypkina, C. Heindl, A. Schindler, M. Bodensteiner, A. V. Virovets, M. Scheer, *Z. Kristallogr.* **2014**, *229*, 735 – 740; b) C. Schwarzmaier, A. Schindler, C. Heindl, S. Scheuermayer, E. V. Peresypkina, A. V. Virovets, M. Neumeier, R. Gschwind, M. Scheer, *Angew. Chem. Int. Ed.* **2013**, *52*, 10896 – 10899; *Angew. Chem.* **2013**, *125*, 11097 – 11100; c) A. Schindler, C. Heindl, G. Balázs, C. Groeger, A. V. Virovets, E. V. Peresypkina, M. Scheer, *Chem. Eur. J.* **2012**, *18*, 829 – 835; d) S. Welsch, C. Groeger, M. Sierka, M. Scheer, *Angew. Chem. Int. Ed.* **2011**, *50*, 1435 – 1438; *Angew. Chem.* **2011**, *123*, 1471 – 1474; e) M. Scheer, A. Schindler, J. Bai, B. P. Johnson, R. Merkle, R. Winter, A. V. Virovets, E. V. Peresypkina, V. A. Blatov, M. Sierka, H. Eckert, *Chem. Eur. J.* **2010**, *16*, 2092 – 2107; f) M. Scheer, A. Schindler, C. Groeger, A. V. Virovets, E. V. Peresypkina, *Angew. Chem. Int. Ed.* **2009**, *48*, 5046 – 5049; *Angew. Chem.* **2009**, *121*, 5148 – 5151; g) M. Scheer, A. Schindler, R. Merkle, B. P. Johnson, M. Linseis, R. Winter, C. E. Anson, A. V. Virovets, *J. Am. Chem. Soc.* **2007**, *129*, 13386 – 13387; h) J. Bai, A. V. Virovets, M. Scheer, *Science* **2003**, *300*, 781 – 783; i) E. Peresypkina, C. Heindl, A. Virovets, H. Brake, E. Mädl, M. Scheer, *Chem. Eur. J.* **2018**, *24*, 2503 – 2508.

[13] O. J. Scherer, T. Brück, G. Wolmershäuser, *Chem. Ber.* **1988**, *121*, 935 – 938.

[14] M. Fleischmann, J. S. Jones, F. P. Gabbai, M. Scheer, *Chem. Sci.* **2015**, *6*, 132 – 139.

[15] O. J. Scherer, T. Hilt, G. Wolmershäuser, *Organometallics* **1998**, *17*, 4110 – 4112.

[16] F. Dielmann, R. Merkle, S. Heinl, M. Scheer, *Z. Naturforsch. B* **2009**, *64b*, 3 – 10.

[17] S. Heinl, G. Balázs, M. Scheer, *Phosphorus Sulfur Silicon Relat. Elem.* **2014**, *189*, 924 – 932.

[18] a) T. P. Gryaznova, S. A. Katsyuba, V. A. Milyukov, O. G. Sinyashin, *J. Organomet. Chem.* **2010**, *695*, 2586 – 2595; b) E. J. Padma Malar, *Eur. J. Inorg. Chem.* **2004**, 2723 – 2732; c) J. Frunzke, M. Lein, G. Frenking, *Organometallics* **2002**, *21*, 3351 – 3359; d) G. Frison, F. Mathey, A. Sevin, *J. Phys. Chem. A* **2002**, *106*, 5653 – 5659.

[19] O. J. Scherer, G. Kemény, G. Wolmershäuser, *Chem. Ber.* **1995**, *128*, 1145 – 1148.

[20] M. Fleischmann, C. Heindl, M. Seidl, G. Balázs, A. V. Virovets, E. V. Peresypkina, M. Tsunoda, F. P. Gabbaï, M. Scheer, *Angew. Chem. Int. Ed.* **2012**, *51*, 9918 – 9921; *Angew. Chem.* **2012**, *124*, 10056 – 10059.

[21] Y.-P. Wang, P. Wu, H.-Y. Cheng, T.-S. Lin, S.-L. Wang, *J. Organomet. Chem.* **2009**, *694*, 285 – 296.

[22] G. L. Hardgrove, D. H. Templeton, *Acta Crystallogr.* **1959**, *12*, 28 – 32.

[23] J. C. A. Bobyens, D. C. Levendis, M. I. Bruce, M. L. Williams, *J. Crystallogr. Spectrosc. Res.* **1986**, *16*, 519 – 524.

[24] P. Seiler, J. D. Dunitz, *Acta Crystallogr. Sect. B* **1982**, *38*, 1741 – 1745.

[25] R. G. Winter, W. E. Geiger, *Organometallics* **1999**, *18*, 1827 – 1833.

[26] All calculations were performed with the Gaussian 09 at the B3LYP/6-31 + + G(3df,3pd) level of theory. The geometry of **1 b** was optimized without symmetry restrains, although the optimized geometry is C_{5v} symmetric. The orbital labelling is according to the C_{5v} point group. Program: Gaussian 09, Revision D.01, M. J. Frisch, G. W. Trucks, H. B. Schlegel, G. E. Scuseria, M. A. Robb, J. R. Cheeseman, G. Scalmani, V. Barone, B. Mennucci, G. A. Petersson, H. Nakatsuji, M. Caricato, X. Li, H. P. Hratchian, A. F. Izmaylov, J. Bloino, G. Zheng, J. L. Sonnenberg, M. Hada, M. Ehara, K. Toyota, R. Fukuda, J. Hasegawa, M. Ishida, T. Nakajima, Y. Honda, O. Kitao, H. Nakai, T. Vreven, J. A. Montgomery, Jr., J. E. Peralta, F. Ogliaro, M. Bearpark, J. J. Heyd, E. Brothers, K. N. Kudin, V. N. Staroverov, T. Keith, R. Kobayashi, J. Normand, K. Raghavachari, A. Rendell, J. C. Burant, S. S. Iyengar, J. Tomasi, M. Cossi, N. Rega, J. M. Millam, M. Klene, J. E. Knox, J. B. Cross, V. Bakken, C. Adamo, J. Jaramillo, R. Gomperts, R. E. Stratmann, O. Yazyev, A. J. Austin, R. Cammi, C. Pomelli, J. W. Ochterski, R. L. Martin, K. Morokuma, V. G. Zakrzewski, G. A. Voth, P. Salvador, J. J. Dannenberg, S. Dapprich, A. D. Daniels, O. Farkas, J. B. Foresman, J. V. Ortiz, J. Cioslowski, and D. J. Fox, Gaussian, Inc., Wallingford CT, **2013**.

[27] H. Krauss, G. Balázs, M. Bodensteiner, M. Scheer, *Chem. Sci.* **2010**, *1*, 337 – 342.

[28] F. Dielmann, C. Heindl, F. Hastreiter, E. V. Peresypkina, A. V. Virovets, R. M. Gschwind, M. Scheer, *Angew. Chem. Int. Ed.* **2014**, *53*, 13605 – 13608.

[29] a) V. A. Blatov, A. P. Shevchenko, D. M. Proserpio, *Cryst. Growth Des.* **2014**, *14*, 3576—3586; b) http://rcsr.anu.edu.au.

[30] J. Schiller, E. Peresypkina, A. Virovets, M. Scheer, *Angew. Chem. Int. Ed.* **2020**, *59*, 13647 – 13650; *Angew. Chem.* **2020**, *132*, 13750 – 13753.

[31] T. G. Mitina, V. A. Blatov, *Cryst. Growth Des.* **2013**, *13*, 1655 – 1664.

[32] M. O'Keeffe, M. A. Peskov, S. J. Ramsden, O. M. Yaghi, *Acts. Chem. Res.* **2008**, *41*, 1782 – 1789.

[33] For X = Cl, Br: After a longer period of time, a small amount of the polymer $[Cp^*Fe(\eta^5\text{-}P_5)(CuX)]_n$[11a] at the bottom as well as, later on, of the 90-vertex supramolecule $[Cp^*Fe(\eta^5\text{-}P_5)]@[\{Cp^*Fe(\eta^5\text{-}P_5)\}_{12}(CuX)_{25}(CH_3CN)_{10}]$[12e] appears.

[34] A. Bondi, *J. Phys. Chem.* **1964**, *68*, 441 – 451.

[35] F. Dielmann, M. Fleischmann, C. Heindl, E. V. Peresypkina, A. V. Virovets, R. M. Gschwind, M. Scheer, *Chem. Eur. J.* **2015**, *21*, 6214 – 6214.

Manuscript received: January 19, 2021
Accepted manuscript online: February 5, 2021
Version of record online: March 11, 2021

